

System Identification and Control of Front-Steered Ackermann Vehicles through Differentiable Physics

Burak M. Gonultas¹, Pratik Mukherjee¹, O. Goktug Poyrazoglu¹ and Volkan Isler¹

Abstract—In this paper, we address the problem of system identification and control of a front-steered vehicle which abides by the Ackermann geometry constraints. This problem arises naturally for on-road and off-road vehicles that require reliable system identification and basic feedback controllers for various applications such as lane keeping and way-point navigation. Traditional system identification requires expensive equipment and is time consuming. In this work we explore the use of differentiable physics for system identification and controller design and make the following contributions: i) We develop a differentiable physics simulator (DPS) to provide a method for the system identification of front-steered class of vehicles whose system parameters are learned using a gradient-based method; ii) We provide results for our gradient-based method that exhibit better sample efficiency in comparison to other gradient-free methods; iii) We validate the learned system parameters by implementing a feedback controller to demonstrate stable lane keeping performance on a *real* front-steered vehicle, the FITENTH; iv) Further, we provide results exhibiting comparable lane keeping behavior for system parameters learned using our gradient-based method with lane keeping behavior of the *actual* system parameters of the FITENTH.

I. INTRODUCTION

Performing experiments with real robots is a difficult, time-consuming issue and often a costly task. To address these issues, there has been growing interest in the robotics community to reduce the gap between simulation and real-world experiments. The intention is to provide roboticists with a virtual environment to develop algorithms and test them on robots in a risk-free manner. However, the trade-off is that validating the performance of algorithms in simulation often does not directly translate to the real-world robots. This primarily occurs because readily available simulation environments are low-fidelity. Current literature have explored two different approaches to tackle the sim-to-real gap issue: i) Developing accurate models of robots and improving the fidelity of simulation environments; ii) Making robot controllers more robust and adaptive to uncertainty in the environment. Source code is available on our project page: <https://github.com/gonultasbu/diffsteered>

Conventionally, improvement on the system model is achieved by traditional *system identification*. Traditional methods for system identification [1] include the *frequency* and *impulse* response methods, where the system parameter is obtained offline using predefined input signals. This typically is a time consuming endeavour and requires the presence of real system which can be expensive and is not

always available. Researchers have also developed online methods for conducting system identification using the recursive least squares method for identifying linear systems [2] and local linear regressors for identifying affine time-varying models [3]. Recently, learning-based approaches have also been applied to improve model fidelity. For instance, [4] performs model identification of mobile *skid-steered* robots using a differentiable physics simulation environment. Our work in this paper extends the work in [4] to front-steered Ackermann type vehicles.



Fig. 1: A feedback controller exhibiting a lane keeping behavior for the FITENTH robot to track a circular trajectory.

On the other hand, when it comes to using controllers to reduce the sim-to-real gap, researchers have worked on developing *robust* and *adaptive* controllers. Hovakimyan and Cao [5] provide a detailed study consisting of the traditional adaptive controllers, as well as modern adaptive controllers that are not only *stable* but also *robust*. However, designing a robust controller that is adaptive by nature requires the design of Lyapunov functions that do not necessarily cater to general systems. Moreover, deriving adaptive controllers and implementing them on real robots is not trivial.

In this work, we focus on the class of mobile robots with front wheel steering. This is an important class of robots which consists of everyday on-road and off-road vehicles used in various applications, i.e., farming, mining, etc. Moreover, with an increase in interest for autonomous vehicles, we realized that there are not many works [6]–[8] that tackle the problem of system identification and control of front-steered mobile robots, and especially using *differentiable physics*

¹ the authors are with the Department of Computer Science and Engineering, University of Minnesota, Minneapolis, MN, 55455, USA {gonul004, mukhe027, poyra002, isler}@umn.edu

simulators (DPS) [9]–[20]. From a controls perspective, there is extensive literature that is provided by the controls community starting with [21]. In [21], Rajamani details *basic* off-the-shelf controllers such as feedback controllers for front-steered vehicles which abide by the Ackermann geometry constraints [22] for the application of lane keeping. Similarly, from a system identification perspective, for mobile robots, recent works such as [4], [23] have addressed solving *simultaneous* system identification and control, but specifically for *skid-steered* vehicles and manipulator type robotic systems, respectively. Realizing this void for system identification and control of front-steered vehicles in the robotics community, which serve a vast array of applications in real-world, we are motivated to provide a robust framework, as shown in Fig. 2, using DPS for system identification and control of front-steered vehicles. The framework in Fig. 2 depicts the system parameter learning using gradient based optimization methods (grey region) offline. Once the parameters are learned in the form of system dynamics equation matrices (A, B), we validate the learned parameters using a *feedback* controller for the application of lane keeping of front-steered Ackermann vehicles (orange region). In this case, we conduct the *system identification* of a readily available front-steered vehicle, the FITENTH, and validate a *traditional* feedback controller for lane keeping application. The FITENTH [24] is a widely used mobile robot in the robotics community for demonstrating autonomous vehicle applications.

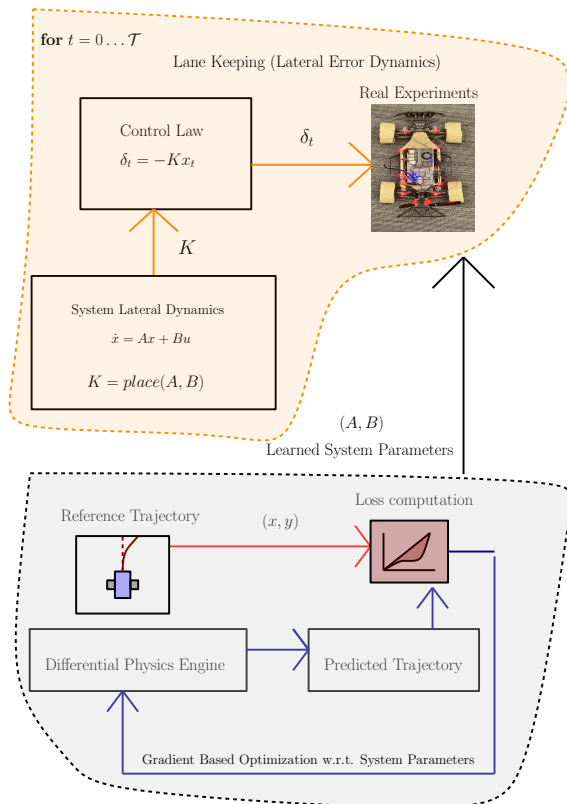


Fig. 2: Overview of our approach depicts offline system identification (grey region) for general systems and feedback control (orange region) for lane keeping application of front-steered FITENTH vehicle.

In this regard, our contributions are fourfold: i) We use differentiable physics simulator (DPS) to provide a method for the system identification of the front-steered FITENTH vehicle whose system parameters are learned using a gradient-based method; ii) We provide results for our gradient-based method that exhibit better sample efficiency in comparison to other gradient-free methods; iii) We validate the learned system parameters by implementing a feedback controller to demonstrate stable lane keeping performance on a *real* front-steered vehicle, the FITENTH; iv) Further, we provide results exhibiting comparable lane keeping behavior for system parameters learned using our gradient-based method with lane keeping behavior of the *actual* system parameters of the FITENTH.

The rest of the paper is organized as follows. Technical background material is summarized in Section II. The formal problem formulation is given in Section III. In Section IV, we provide extensive details on our method for system identification. Finally, we provide simulation results in Section V and experimental results with FITENTH in Section VI and conclude the paper in Section VII.

II. TECHNICAL BACKGROUND

In this section, we briefly review the theory behind the front-steered vehicle lateral *error* dynamics derived in [21] and discuss the framework of DPS used for our simulations.

A. Vehicle lateral Dynamics

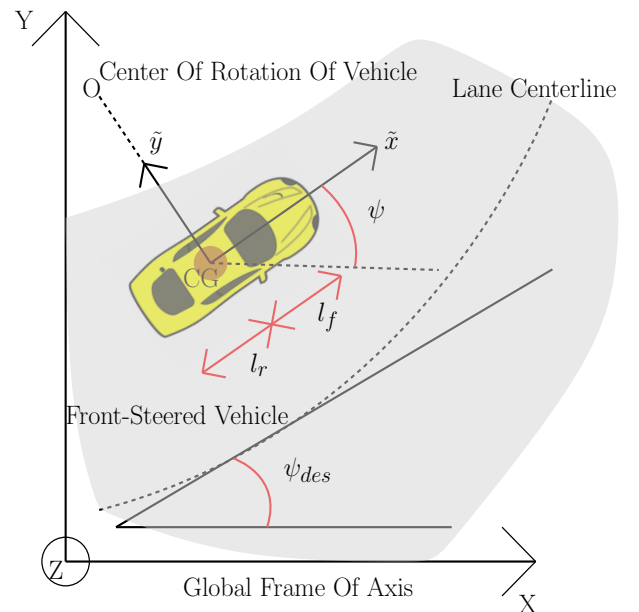


Fig. 3: A lateral lane keeping system for a front-steered vehicle.

Fig. 3 shows a simplified linear two-degrees of freedom (2-DOF) bicycle model of the vehicle lateral dynamics derived in [21]. 2-DOF are ψ , the vehicle yaw angle, and y , the lateral position with respect to the center of the rotation of the vehicle O . The yaw angle is considered as the angle between horizontal *vehicle body frame* axis of the vehicle, (\tilde{x}), and

the global horizontal axis, (X). The *constant* longitudinal velocity of the vehicle at its center of gravity (CG) is denoted by V_x and the mass of the vehicle is denoted by m . The distances of the front and rear tires from the CG are shown by l_f , l_r , respectively, and the front and rear tire cornering stiffness are denoted by C_{af} and C_{ar} , respectively. The steering angle is denoted by δ which also serves as the control signal when a controller is implemented and the yaw moment of inertia of the vehicle is denoted by I_z . Considering the lateral position, yaw angle, and their derivatives as the state variables, and using the Newton's second law for the motion along the *vehicle body frame* \tilde{y} -axis, the state space model of lateral vehicle dynamics is derived in [21].

The error dynamics is written with two error variables : e_1 , which is the distance between the CG of the vehicle from the center line of the lane; e_2 , which is the orientation error of the vehicle with respect to the desired yaw angle ψ_{des} . Assuming the radius of the road is R , the rate of change of the desired orientation of the vehicle can be defined as $\dot{\psi}_{des} = \frac{V_x}{R}$. The tracking or lane keeping objective of the lateral control problem is expressed as a problem of stabilizing the following *error* dynamics at the origin.

$$\begin{aligned} \frac{d}{dt} \begin{bmatrix} e_1 \\ \dot{e}_1 \\ e_2 \\ \dot{e}_2 \end{bmatrix} &= \underbrace{\begin{bmatrix} 0 & 1 & 0 & 0 \\ 0 & -\frac{2C_{af}+2C_{ar}}{mV_x} & \frac{2C_{af}+2C_{ar}}{m} & -\frac{2C_{af}l_f-2C_{ar}l_r}{mV_x} \\ 0 & 0 & 0 & 1 \\ 0 & -\frac{2C_{af}l_f-2C_{ar}l_r}{I_zV_x} & \frac{2C_{af}l_f-2C_{ar}l_r}{I_z} & -\frac{2C_{af}l_f^2+2C_{ar}l_r^2}{I_zV_x} \end{bmatrix}}_A \\ &\times \underbrace{\begin{bmatrix} e_1 \\ \dot{e}_1 \\ e_2 \\ \dot{e}_2 \end{bmatrix}}_x + \underbrace{\begin{bmatrix} 0 \\ \frac{2C_{af}}{m} \\ 0 \\ \frac{2C_{af}l_f}{I_z} \end{bmatrix}}_{B_1} \underbrace{\delta}_u + \underbrace{\begin{bmatrix} 0 \\ -V_x - \frac{2C_{af}l_f-2C_{ar}}{mV_x} \\ 0 \\ -\frac{2C_{af}l_f^2+2C_{ar}l_r^2}{I_zV_x} \end{bmatrix}}_{B_2} \dot{\psi}_{des} \end{aligned} \quad (1)$$

Therefore, the above state-space form in (1) can be represented in the *general* state space form as

$$\dot{x}(t) = Ax(t) + B_1(u(t)) + B_2\dot{\psi}_{des} \quad (2)$$

where $x(t) \in \mathbb{R}^n$, $t \geq 0$ is a state vector, $u(t) \in \mathbb{R}^m$, $t \geq 0$ is the control input which in this case is the steering angle δ . The elements of $A \in \mathbb{R}^{n \times n}$, $B_1, B_2 \in \mathbb{R}^{n \times m}$ matrices are generally considered known, but in our case we obtain the elements of matrices using system identification and we assume pair (A, B_1) is controllable. We also provide the definition of a closed-loop system.

Definition 1: The closed-loop system is defined as the system described by equation (2), where $u(t) = \delta_t, \forall t$, is the steering angle input to the system generated by a feedback controller .

B. Differentiable Physics Simulator (DPS)

Differentiable physics simulators provide analytical gradients for physical systems, which may be used for learning-based solutions such as solving inverse problems, system

identification and controller design. Enabled by the recent developments in automatic differentiation literature [25]–[30], a number of differentiable simulators have been proposed [9]–[20]. While these simulators all aim to provide analytical gradients for learning-based methods, the variance in terms of supported features is high. In this paper, PyTorch [25] library is used to develop the differentiable physics engine, which is differentiable with respect to the dynamic model parameters and control inputs of front-steered Ackermann vehicles.

The dynamic model, which is represented by a state space model as shown in (3), consists of the following states $x_1 = s_x, x_2 = s_y, x_3 = \delta, x_4 = v, x_5 = \psi, x_6 = \dot{\psi}, x_7 = \beta$.

$$\begin{aligned} \dot{x}_1 &= x_4 \cos(x_5 + x_7) \\ \dot{x}_2 &= x_4 \sin(x_5 + x_7) \\ \dot{x}_3 &= f_{steer}(x_3, u_1) \\ \dot{x}_4 &= f_{acc}(x_4, u_2) \\ \dot{x}_5 &= x_6 \\ \dot{x}_6 &= \frac{\mu m}{I_z(l_r + l_f)} (l_f C_{s,f}(gl_r - u_2 h_{cg})x_3 + (l_r C_{S,r} \dots \\ &\quad (gl_f + u_2 h_{cg}) - l_f C_{S,f}(gl_r - u_2 h_{cg}))x_7 \dots \\ &\quad - (l_f^2 C_{S,f}(gl_r - u_2 h_{cg})x_3 + l_r^2 C_{S,r}(gl_f + u_2 h_{cg})) \frac{x_6}{x_4}) \\ \dot{x}_7 &= \frac{\mu}{x_4(l_r + l_f)} (C_{s,f}(gl_r - u_2 h_{cg})x_3 - (C_{S,r} \dots \\ &\quad (gl_f + u_2 h_{cg}) + C_{S,f}(gl_r - u_2 h_{cg}))x_7 \dots \\ &\quad + (C_{S,r}(gl_f - u_2 h_{cg})l_r) - C_{S,f}(gl_r - u_2 h_{cg})l_f) \frac{x_6}{x_4}) - x_6 \end{aligned} \quad (3)$$

where s_x is the x position in global coordinates in meters, s_y is the y position in global coordinates in meters, v is the longitudinal velocity in m/s, and β is the slip angle at the vehicle center in radians. Defined vehicle parameters are as follows: h_{cg} is the center of gravity height of total mass in meters. μ is the friction coefficient, $C_{S,f}$ and $C_{S,r}$ are tire cornering stiffness coefficients for front and rear wheels in $1/rad$. Inputs are defined as u_1 representing the steering velocity and u_2 representing the longitudinal acceleration. The vehicle parameters and definitions are compatible between equations (1) and (3) except for the angles and related coefficients. Eq. (1) uses degrees instead of radians, therefore cornering stiffness coefficients from Eq. (3) must be converted to cornering stiffness values which are in degrees. The relation between cornering stiffness and the corresponding coefficient is as follows:

$$C_{ai} = \mu C_{S,i} F_{z,i} \quad (4)$$

Where the subscript i assigns a tire or axle to the front and the rear. Therefore, $F_{z,i}$ becomes the vertical force on the front or rear axle in N .

III. PROBLEM FORMULATION

At a high-level we want to conduct system identification and learn a dynamic model for front-steered vehicles. Therefore, we formulate the system identification problem as a

general optimization problem in terms of identified system dynamic parameters in a DPS environment as the decision variables. The optimization goal is to minimize the gap between the trajectory of the real system and the simulated system. To verify the task based sim2real performance of the identified system parameters, we use a *feedback* controller of the type used in [21] as the basic controller for lane keeping with the error dynamics shown in state-space form in Eq. (1).

In the following sub-sections we further elaborate on our *problem definition*

A. Task Representation

Given a front steered vehicle with center of gravity CG , its generalized position at time t in real world is defined as a 2-tuple of Cartesian coordinates (x_t^{real}, y_t^{real}) . Similarly, its generalized position at time t in simulation is defined as (x_t^{sim}, y_t^{sim}) . In simulation, the front-steered vehicle defined by the dynamic equations (1) is expected to follow a trajectory that is as close to the real-world trajectory as possible for the same set of control inputs with constant longitudinal velocity V_x . For the real world performance, according to the feedback controller implementation in [21] the steady state values of e_1 and e_2 may be non-zero but should converge close to zero.

B. Model Identification

The problem formulation becomes an optimization problem of minimizing the gap between the simulated trajectory and the real robot trajectory as follows:

$$\min_{\hat{P}} \hat{\mathcal{L}}(r, \hat{r}) \quad (5)$$

where $\hat{\mathcal{L}}$ representing the gap between the real and simulated trajectories \hat{r} and r respectively.

C. Verifying the Control Law in Real World

The open-loop matrix A may have eigenvalues at the origin and be unstable. Using the state feedback law, the eigenvalues of the closed-loop matrix $(A - BK)$ can be placed at desired locations. The closed-loop system, as defined in Definition 1, using this state feedback controller is therefore:

$$\dot{x} = (A - B_1K)x + B_2\dot{\Psi}_{des} \quad (6)$$

To compute the feedback matrix K , the pole placement algorithm [31] is used.

$$K = place(A, B_1, P) \quad (7)$$

Where the vector P , which is user defined, defines the desired pole locations such that the eigenvalues of the matrix $(A - B_1K)$ are negative, non-zero real numbers, satisfying the *full state feedback* system stability condition. From Eq. (1) it is observable that the matrices A and B_1 are defined by the front-steered vehicle dynamic parameters m , l_f , l_r , C_{af} and C_{ar} . We hypothesize that correctly identifying the set of system dynamic parameters in Eq. (1) would yield the gain vector K that would make the steady state values of e_1 and e_2 converge close to zero in real world experiments.



Fig. 4: FITENTH with a lower tire friction configuration. The rubber tires are wrapped using a tape that has less grip on carpet surface.

IV. METHOD

A. Vehicle Data Collection

The vehicle was driven indoors with Phasespace X2E LED motion capture markers attached on top of it for 6 DoF state estimation. The vehicle was autonomously operated through its ROS interface [32] for 6-10 seconds. To test how general our method is, we also wrapped the vehicle tires with tape for a second set of experiments, which is expected to reduce the friction between the vehicle tires and the ground (Fig. 4). For simplicity, a total of 16 circular trajectories were collected for training equally split between left and right turns at maximum steering angle at 1 m/s velocity for both friction conditions. To preserve compatibility with the state-space definition provided in Eq. (2), we do not apply any steering velocity or longitudinal acceleration commands which is represented as $u_1 = 0$ and $u_2 = 0$. Instead, we are directly modifying the states x_3 and x_4 , which are the steering angle and longitudinal velocity, respectively.

B. Loss Function

The loss function needs to minimize the gap between the simulated and the real robot trajectory:

$$\mathcal{L}_{dtw} = dtw(r, \hat{r}) \quad (8)$$

where dtw refers to the differentiable implementation of Dynamic Time Warping [33]–[35] algorithm. In practice, Dynamic Time Warping does not penalize the scale difference between trajectories enough, therefore it needs to be combined with another loss term to prevent trajectories of similar shapes but large scale differences. For that purpose, we use the chamfer distance as the second loss term.

$$\mathcal{L}_{cd} = cd(r, \hat{r}) \quad (9)$$

A weighted linear combination of \mathcal{L}_{dtw} and \mathcal{L}_{cd} is proposed as the actual loss function:

$$\mathcal{L} = \mathcal{L}_{dtw} + \lambda \mathcal{L}_{cd} \quad (10)$$

where the weight is empirically determined as $\lambda = 100$.

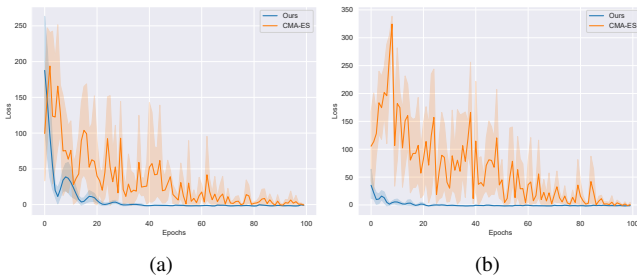


Fig. 5: The loss trend for model identification. Both methods use the analytical methods but only our method makes use of the analytical gradients provided by our differentiable physics engine. Analytical gradients provide higher sample efficiency and the training converges in far fewer iterations, (a) shows the model identification of the F1TENTH vehicle with standard tire configuration (b) shows the model identification for the lower friction configuration.

V. SIMULATION RESULTS

In this section, we first compare our gradient-based method to a gradient-free baseline. The front-steered vehicle was simulated through our differentiable physics engine with timestep size of 0.002 s. Our simulator implements the nonlinear dynamics given in Eq. (3) and adopted by the official F1TENTH simulator [24]. h_{cg} is fixed as 0.074 meters, I_z is fixed as 0.04712 $kg.m^2$ m is measured at 3.1 kg . The coefficient of friction between the vehicle wheels and the ground was set to $\mu = 1.0489$ and the steering angles were clipped at each timestep, to remain in the interval: $[-0.34, 0.34]$ $rads$ in accordance with the physical model properties. The velocity was kept constant at 1 m/s . In our experiments, we are looking to identify the following model parameters: l_f , l_r , $C_{S,f}$, $C_{S,r}$. For training, batch size is set to 4 for Adam optimizer [36]. Loss and parameter figures are plotted as the average of 5 separate training rounds with uniformly sampled random initial parameters. For the baseline, gradient-free optimizer CMA-ES [37] is used for optimizations from the Optuna library [38].

We present the loss curves for gradient-based and gradient-free gain optimizations in Fig. 5 for 100 epochs. Compared to the gradient-free baseline, our gradient-based method provides much higher sample-efficiency and a more regular loss curve enabled by the analytical gradients for standard and lower friction tire configurations both. The effect of the analytical gradients is particularly evident in the first few epochs where gradient-based methods have to initially explore the search space. In Table I we present the model parameters estimated by the gradient-based and gradient-free optimization methods averaged over 5 initializations sampled uniformly at random. The first two rows demonstrate the values provided by the official implementation of the F1TENTH vehicle and our method’s results, respectively. The results suggest that our method is able to closely match more sophisticated system identification methods through a simpler procedure. Per Eq. (3), for a simulation with fixed friction

TABLE I: ESTIMATED MODEL PARAMETERS

Estimation Method	l_f	l_r	$C_{S,f}$	$C_{S,r}$
True	0.159	0.171	4.728	5.546
Ours	0.142	0.171	5.909	4.767
Ours(low friction)	0.161	0.143	5.113	4.988
CMA-ES	0.127	0.194	7.442	6.147
CMA-ES(low friction)	0.155	0.143	6.823	8.960

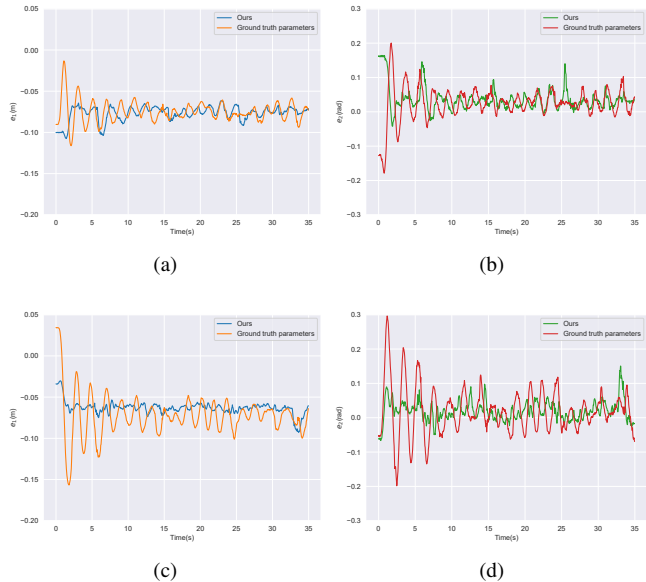


Fig. 6: Error profile of e_1 in meters and e_2 in radians for (a) and (b) F1TENTH vehicle with standard tire configuration (c) and (d) with the lower friction configuration. In both cases, error profiles confirm that the feedback controller using parameters identified through our method has comparable performance w.r.t the ground truth parameters identified in the official implementation [24].

coefficient, our hypothesis was to observe a significantly lower cornering stiffness coefficient for the lower friction configuration. In the third row of Table I our method’s results are presented. They are a bit unexpected as the cornering stiffness values are higher. We hypothesize that experiments using acceleration and steering velocity commands would get closer to the friction limits of the vehicle would make this change of parameters more observable.

VI. REAL WORLD EXPERIMENT RESULTS

For the real world experiments, the feedback controller presented in Eq. (6) is used. The poles were set as $P = [-2 + 2j, -2 - 2j, -150 + 15j, -150 - 15j]$ since left hand side pole placement is necessary for the stability of the controller. The error profiles presented in Fig. 6 for e_1 and e_2 demonstrate that the identified models are transferable to real systems and optimized controllers show similar performance. As discussed in Section V, two set of experiments were conducted. In 6a and 6b, for the standard tire configuration case, the error profiles demonstrate comparable performance

to the ground truth parameters identified in the official implementation with the identified system parameters in our experiments. For the lower friction case, in 6c and 6d, the identified model for the lower friction case performs well, however the identified standard parameters do not seem to suffer significantly and the controller performance is still robust. We attribute the robustness of the default controller performance under lower friction setting to the relatively conservative longitudinal velocity and feedback mechanism's ability to compensate small model identification errors, evident in Sec V, where identified model parameters are relatively similar. For further details on our experimental results, please refer to the submitted video attachment.

VII. CONCLUSIONS AND FUTURE DIRECTIONS

Front-steered vehicles constitute the majority of driving equipment. In this paper we presented a method for system-identification and control of front-steered vehicles and demonstrated our approach on the FITENTH vehicle, which abides by the Ackerman geometry constraints, using a differentiable physics engine combined with gradient-based optimization methods. With the help of the analytical gradients provided by the differentiable physics engine, our method converges in far fewer iterations compared to the gradient-free baseline. Our proposed method identifies the unknown parameters of the system as well as executes a stable feedback controller used to achieve lane keeping. We provided experimental results using an FITENTH vehicle exhibiting comparable lane keeping behavior for system parameters learned using our gradient-based method with lane keeping behavior of the *actual* system parameters of the FITENTH.

For the future, we will work on implementing an online system identification and controller methodology for front-steered Ackermann vehicles.

REFERENCES

- [1] I. Sa, M. Kamel, R. Khanna, M. Popović, J. Nieto, and R. Siegwart, "Dynamic system identification, and control for a cost-effective and open-source multi-rotor mav," in *Field and Service Robotics*. Springer, 2018, pp. 605–620.
- [2] M. Kaess, A. Ranganathan, and F. Dellaert, "isam: Incremental smoothing and mapping," *IEEE Transactions on Robotics*, vol. 24, no. 6, pp. 1365–1378, 2008.
- [3] U. Rosolia and F. Borrelli, "Learning how to autonomously race a car: a predictive control approach," *IEEE Transactions on Control Systems Technology*, vol. 28, no. 6, pp. 2713–2719, 2019.
- [4] E. Granados, A. Boularias, K. Bekris, and M. Aanjaneya, "Model identification and control of a low-cost mobile robot with omnidirectional wheels using differentiable physics," in *2022 International Conference on Robotics and Automation (ICRA)*. IEEE, 2022, pp. 1358–1364.
- [5] N. Hovakimyan and C. Cao, \mathcal{L}_1 adaptive control theory: Guaranteed robustness with fast adaptation. SIAM, 2010.
- [6] Z. Yu and J. Wang, "Simultaneous estimation of vehicle's center of gravity and inertial parameters based on ackermann's steering geometry," *Journal of Dynamic Systems, Measurement, and Control*, vol. 139, no. 3, 2017.
- [7] S. Carpin, M. Lewis, J. Wang, S. Balakirsky, and C. Scrapper, "Usarsim: a robot simulator for research and education," in *Proceedings 2007 IEEE International Conference on Robotics and Automation*. IEEE, 2007, pp. 1400–1405.
- [8] G. Boer, "A physical multi-body car model using 3-d (screw) bond graphs," Master's thesis, University of Twente, 2002.
- [9] Y. Hu, L. Anderson, T.-M. Li, Q. Sun, N. Carr, J. Ragan-Kelley, and F. Durand, "DiffTaichi: Differentiable programming for physical simulation," *arXiv preprint arXiv:1910.00935*, 2019.
- [10] C. D. Freeman, E. Frey, A. Raichuk, S. Girgin, I. Mordatch, and O. Bachem, "Brax—a differentiable physics engine for large scale rigid body simulation," *arXiv preprint arXiv:2106.13281*, 2021.
- [11] F. Röhrbein and E. Uchibe, "A differentiable physics engine for deep learning in robotics," *Frontiers in Neurobotics—Editor's Pick 2021*, 2021.
- [12] E. Heiden, D. Millard, H. Zhang, and G. S. Sukhatme, "Interactive differentiable simulation," *arXiv preprint arXiv:1905.10706*, 2019.
- [13] F. de Avila Belbute-Peres, K. Smith, K. Allen, J. Tenenbaum, and J. Z. Kolter, "End-to-end differentiable physics for learning and control," *Advances in neural information processing systems*, vol. 31, 2018.
- [14] J. Degraeve, M. Hermans, J. Dambre, *et al.*, "A differentiable physics engine for deep learning in robotics," *Frontiers in neurobotics*, p. 6, 2019.
- [15] M. Geilinger, D. Hahn, J. Zehnder, M. Bächer, B. Thomaszewski, and S. Coros, "Add: Analytically differentiable dynamics for multi-body systems with frictional contact," *ACM Transactions on Graphics (TOG)*, vol. 39, no. 6, pp. 1–15, 2020.
- [16] Y.-L. Qiao, J. Liang, V. Koltun, and M. C. Lin, "Scalable differentiable physics for learning and control," *arXiv preprint arXiv:2007.02168*, 2020.
- [17] M. A. Toussaint, K. R. Allen, K. A. Smith, and J. B. Tenenbaum, "Differentiable physics and stable modes for tool-use and manipulation planning," 2018.
- [18] C. Schenck and D. Fox, "Spnets: Differentiable fluid dynamics for deep neural networks," in *Conference on Robot Learning*. PMLR, 2018, pp. 317–335.
- [19] J. Liang, M. Lin, and V. Koltun, "Differentiable cloth simulation for inverse problems," *Advances in Neural Information Processing Systems*, vol. 32, 2019.
- [20] Y. Hu, J. Liu, A. Spielberg, J. B. Tenenbaum, W. T. Freeman, J. Wu, D. Rus, and W. Matusik, "Chainqueen: A real-time differentiable physical simulator for soft robotics," in *2019 International conference on robotics and automation (ICRA)*. IEEE, 2019, pp. 6265–6271.
- [21] R. Rajamani, *Vehicle dynamics and control*. Springer Science & Business Media, 2011.
- [22] J. Ackermann, "Robust control prevents car skidding," *IEEE Control systems magazine*, vol. 17, no. 3, pp. 23–31, 1997.
- [23] S. Chen, K. Werling, and C. K. Liu, "Real-time model predictive control and system identification using differentiable physics simulation," *arXiv preprint arXiv:2202.09834*, 2022.
- [24] M. O'Kelly, H. Zheng, D. Karthik, and R. Mangharam, "FITenth: An open-source evaluation environment for continuous control and reinforcement learning," *Proceedings of Machine Learning Research*, vol. 123, 2020.
- [25] A. Paszke, S. Gross, F. Massa, A. Lerer, J. Bradbury, G. Chanan, T. Killeen, Z. Lin, N. Gimelshein, L. Antiga, *et al.*, "Pytorch: An imperative style, high-performance deep learning library," *Advances in neural information processing systems*, vol. 32, 2019.
- [26] M. Abadi, P. Barham, J. Chen, Z. Chen, A. Davis, J. Dean, M. Devin, S. Ghemawat, G. Irving, M. Isard, *et al.*, "{TensorFlow}: a system for {Large-Scale} machine learning," in *12th USENIX symposium on operating systems design and implementation (OSDI 16)*, 2016, pp. 265–283.
- [27] R. Al-Rfou, G. Alain, A. Almahairi, C. Angermueller, D. Bahdanau, N. Ballas, F. Bastien, J. Bayer, A. Belikov, A. Belopolsky, *et al.*, "Theano: A python framework for fast computation of mathematical expressions," *arXiv e-prints*, pp. arXiv–1605, 2016.
- [28] Y. Hu, T.-M. Li, L. Anderson, J. Ragan-Kelley, and F. Durand, "Taichi: a language for high-performance computation on spatially sparse data structures," *ACM Transactions on Graphics (TOG)*, vol. 38, no. 6, pp. 1–16, 2019.
- [29] B. M. Bell, "Cppad: a package for c++ algorithmic differentiation," *Computational Infrastructure for Operations Research*, vol. 57, no. 10, 2012.
- [30] J. Bradbury, R. Frostig, P. Hawkins, M. J. Johnson, C. Leary, D. Maclaurin, G. Necula, A. Paszke, J. VanderPlas, S. Wanderman-Milne, *et al.*, "Jax: composable transformations of python+ numpy programs," *Version 0.2*, vol. 5, pp. 14–24, 2018.
- [31] J. Kautsky, N. K. Nichols, and P. Van Dooren, "Robust pole assignment in linear state feedback," *International Journal of control*, vol. 41, no. 5, pp. 1129–1155, 1985.

- [32] M. Quigley, K. Conley, B. Gerkey, J. Faust, T. Foote, J. Leibs, R. Wheeler, A. Y. Ng, *et al.*, “Ros: an open-source robot operating system,” in *ICRA workshop on open source software*, vol. 3, no. 3.2. Kobe, Japan, 2009, p. 5.
- [33] M. Müller, “Dynamic time warping,” *Information retrieval for music and motion*, pp. 69–84, 2007.
- [34] M. Maghoumi, “Deep Recurrent Networks for Gesture Recognition and Synthesis,” Ph.D. dissertation, University of Central Florida Orlando, Florida, 2020.
- [35] M. Cuturi and M. Blondel, “Soft-dtw: a differentiable loss function for time-series,” in *International conference on machine learning*. PMLR, 2017, pp. 894–903.
- [36] D. P. Kingma and J. Ba, “Adam: A method for stochastic optimization,” *arXiv preprint arXiv:1412.6980*, 2014.
- [37] N. Hansen, “The cma evolution strategy: A tutorial,” *arXiv preprint arXiv:1604.00772*, 2016.
- [38] T. Akiba, S. Sano, T. Yanase, T. Ohta, and M. Koyama, “Optuna: A next-generation hyperparameter optimization framework,” in *Proceedings of the 25th ACM SIGKDD international conference on knowledge discovery & data mining*, 2019, pp. 2623–2631.